

Short-range, Non-contact Detection of Surface Contamination Using Raman Lidar

Arthur J. Sedlacek, III* and Mark D. Ray§

Brookhaven National Laboratory, Building 703, Upton, NY 11973

and

N. S. Higdon† and D. A. Richter

ITT Industries, Advanced Engineering & Sciences Division, 6400 Uptown Blvd., Suite 300E

Albuquerque, NM, 87110

Abstract

The application of a novel mini-Raman Lidar to the standoff detection and identification of chemical spills is discussed. The new chemical sensor combines the spectral fingerprinting of solar-blind UV Raman spectroscopy with the principles of lidar to open a new venue of short-range (meters to tens of meters), non-contact detection and identification of unknown substances on surfaces. In addition to discussing experimental results collected with a “proof-of-principle” system, a next generation system, currently under development, is also presented

Keywords: Raman, lidar, surface, portable, chemical sensor, contamination, non-contact, standoff, in-situ, MRLS, LISA

Introduction

Emergency response, environmental monitoring/remediation, and forensic investigations often require rapid, *in situ*, real-time detection and identification of bulk amounts of substances on surfaces. Optical spectroscopic methods are well suited for this task, as evidenced by the availability of portable chemical sensors based on laser-induced fluorescence¹, infrared absorption², and Raman scattering^{3,4,5,6}.



Figure 1. The Mini-Raman lidar System (MRLS)

In response to this need Brookhaven National Laboratory (BNL) developed the Mini-Raman Lidar System (MRLS)⁷, which served as a “proof-of-principle” device specifically designed to address the problem of detection and identification of ground/surface contamination. The MRLS, pictured in Figure 1, accomplished this objective by utilizing both the spectral fingerprinting of Raman spectroscopy and the principles of lidar. The fundamental difference between the MRLS and current portable Raman detectors is the capability of standoff, non-contact detection; that is, the substances are analyzed *in situ* at distances of meters to tens of meters without being touched. This technology is fundamentally different in that these other instruments require that a sample be collected or that some part of the sensor be brought into close proximity to the substance prior to identification, as is the case with fiber optic-based sensors. For those that respond to unknown chemical spills, this

* sedlacek@bnl.gov

§ Present Address; BF Goodrich Aerospace

† scott.higdon@itt.com

limitation necessitates following "worst-case" safety protocols until the substances are conclusively identified. The ability to do standoff, non-contact detection is desirable, especially if the substances are suspected to be toxic.

While the MRLS technology is based on the architecture of Raman lidar, it, and its follow-on sensors currently under development (*infra vide*), are distinct from classic lidar systems because they are specialized for (i) the detection of substances on surfaces at (ii) short ranges. Typically, lidar systems are used to range as well as detect airborne constituents and particles at kilometer distances. Hence, this novel short-range, non-contact remote sensing technique cannot be properly described as a form of lidar.

Historically, while Raman lidar has been successfully used to measure percent-level atmospheric constituents at kilometer distances, its ability to remotely measure trace-level airborne pollutants is problematic due to the inherently small Raman cross-sections.⁸ However, at short standoff ranges, the tremendous increase in signal due to the $1/R^2$ effect makes Raman detection practical. Theoretical analysis and laboratory measurements of Raman scattering from chemical agents and compounds at short ranges have been performed by other researchers.^{5,8,9} The MRLS represents the first operational standoff detection system which has been successfully demonstrated both in the laboratory and through field trials such as the 1997 New York City Intra-Agency Chemical Exercise.

In September 2000, BNL and ITT cooperatively participated in the Joint Chemical Field Trials (sensor field evaluations for the Restoration of Operations (RestOps) Advanced Concept Technology Demonstration (ACTD)) at Dugway Proving Ground. BNL and ITT deployed the MRLS to Dugway and conducted a series of measurements of chemical agent simulants and actual chemical agents during a 2-week period.¹⁰ The MRLS successfully detected and identified chemical agent simulants at stand-off distances of ~2.5 m on several different surfaces at varying concentration levels, but not down to the 0.5 g/m² level required for military reconnaissance systems. This performance limitation of the current MRLS was expected, since it was designed for a broader range of applications and not optimized specifically for these tests.

In addition to the groundbreaking work using the MRLS work, BNL and ITT have also been collaborating on the transitioning of the mini-Raman lidar technology for military sensing missions. This effort, known as Laser Interrogation of Surface Agents (LISA) builds upon the work conducted at BNL under DOE sponsorship and has as its goal, the testing and deployment of a fieldable system operable by non-experts. Finally, in addition to short-range detection and identification of chemical spills, BNL also has developed and successfully tested a larger system mounted in a van, called the Mobile Raman Lidar Van (MRLV) for detection at ranges over 500 meters.¹¹

Experimental Background

Since the experimental details of the MRLS have been published elsewhere⁷ only those subsystems relevant to the present discussion will be highlighted here. The "proof-of-principle" MRLS consists of a 50 lb. tripod-mounted optical head measuring 10" x 18" x 42" which is connected, via an umbilical cord, to a 24" x 24" x 36" power supply cart. The entire system, including the on-board water chiller, consumes about 800 W of line power. The entire optical system is mounted rigidly to a single platform to preserve the alignment of all of the components. Tilting the entire head varies the pointing direction of the MRLS.

The transmitter is a small, flashlamp-pumped 266 nm Nd:YAG laser (New Wave Lase II; 20 Hz, 7 mJ/pulse, 6 ns pulsewidth). The beam diameter is 3 mm at the exit aperture, with a divergence of 1 mrad x 2 mrad. The receiver is a 6-inch diameter, f/4 Newtonian telescope that is coaxial with the transmitted laser beam. The coaxial design ensures that the surface illuminated by the UV laser beam remains within the field-of-view of the telescope. Both the scattered red light and the UV light are collected by the primary. The secondary of the Newtonian is rigidly mounted, while the 6-inch primary is mounted on a rail glide driven by a lead screw with a DC servomotor. Variations in the target distance (as measured by the range finder) require that the primary adjust its position to keep the image plane at the entrance slit of the analyzing spectrometer. The secondary is a dielectric 266 nm mirror that passes most of the 635 nm light (range finder) while reflecting the UV light into the spectrometer. The collected red light is routed back to the collection window of the range finder. The distance determined by the range finder is independent of the light return path, so no correction for the current position of the primary is required. Currently, the shortest standoff distance is two meters due to the limit of the travel range of the primary.

To prevent the strong elastically scattered laser light from obscuring the weaker Raman signals, a sharp-cut edge filter (Barr Associates) is placed between the receiver telescope and the spectrometer to reject the 266 nm light collected by the

telescope. The rejection ratio is $10^5:1$, with the 50% transmission point located 350 cm^{-1} to the red of the 266 nm line. The transmission at the Raman-shifted wavelengths is about 80%.

The analyzing spectrometer is a 0.25 m , $f/4$ spectrometer designed to be compact and lightweight yet have sufficient resolution and stray light rejection to collect Raman spectra. The spectrometer, as well as the telescope, is built directly onto the optical mounting plate. The grating is a 2380 groove/mm concave holographic grating (American Holographic). This novel spectrometer uses a single curved optic to reduce the complexity of the alignment. The spectrometer has no moving parts, so that the spectral window is fixed. An optical array detector captures the Raman spectrum from 600 cm^{-1} to 4000 cm^{-1} to the red of the laser line. Small adjustments in the angle of the grating can shift the position of the spectral window. The spectral resolution of the MRLS is 22 cm^{-1} full-width half-maximum (FWHM).

The array detector is a gated, intensified CCD (Andor InstaSpec V). The intensifier acts as an optical amplifier to raise small light signals above the dark noise of the CCD chip. It also serves effectively as a fast shutter (10 ns minimum gatewidth) that can be operated in sync with the pulsed laser. Hence, for every second of signal integration time, the shutter can be open for as little as 200 ns . The CCD array is 1024×256 pixels, with the Raman spectrum dispersed along the longer (horizontal) dimension. The signal in the 256 vertical pixels is binned to produce a single channel signal. A plot of binned signal versus channel number forms the Raman spectrum. The channel numbers are then calibrated to the Raman shift in cm^{-1} . Data acquisition and analysis are controlled by a laptop computer (Gateway Solo with LabVIEW software). A library of Raman spectra of pure samples taken with the MRLS is stored for use in substance identification.

MRLS Results and Discussion

Acetonitrile is used as a test chemical due to its low absorption cross-section in the $260\text{-}300\text{ nm}$ region. As expected, sensitivity estimates based on acetonitrile scale linearly with the sample pathlength. In addition, the cross-sections of the 918 cm^{-1} and 2249 cm^{-1} Raman modes have been measured at 220 nm and 280 nm and can be interpolated fairly reliably using the ν^4 -relationship for scattering in the dipole approximation.¹² For excitation at 266 nm , the Raman cross-sections are $2 \times 10^{-29}\text{ cm}^2/\text{molecule-ster}$ for the mode at 918 cm^{-1} and $1.4 \times 10^{-28}\text{ cm}^2/\text{molecule-ster}$ for the mode at 2249 cm^{-1} .

One of the strengths of Raman spectroscopy is its ability to identify substances in the solid as well as gaseous and liquid phase. To illustrate this point, we placed a film of acetonitrile onto the Teflon sheet and probed it with the MRLS. The top trace in Figure 2 shows the Raman spectrum of a Teflon sheet while the middle trace shows the spectrum of a thin film of acetonitrile on the Teflon sheet. The lower trace is the spectrum of the pure acetonitrile generated by subtracting the middle trace from the upper trace. The thickness of the acetonitrile film is calculated from a determination of the acetonitrile weighting coefficient and, for the present case, is found to be approximately $90\text{ }\mu\text{m}$. In principle, a mixture of many chemicals can be identified and quantified. The fundamental limitations are the spectral resolution of the spectrometer and the dynamic range of the array detector (40 dB).

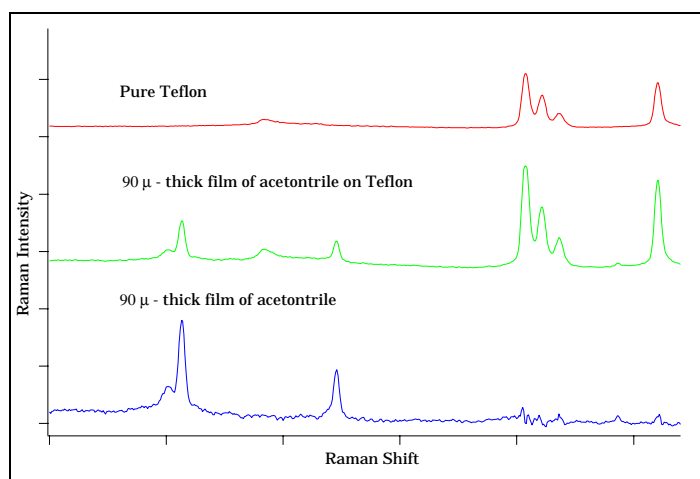


Figure 2. Raman spectrum acetonitrile film on Teflon surface at a standoff distance of 3 m for a signal integration time of 5 s . From the weighting coefficient for acetonitrile, the thickness of the film is estimated to be $90\text{ }\mu\text{m}$. See text for details.

The MRLS has also demonstrated the ability to acquire the unique spectral signature of a chemical species on a variety of surfaces. This is illustrated in Figure 3 which shows Raman spectra for SF-96, a VX surrogate, as a pure sample in a quartz cell and when deposited on three different surfaces. For clarity, the background spectra for the surfaces have been subtracted to yield the spectra for SF-96 alone.

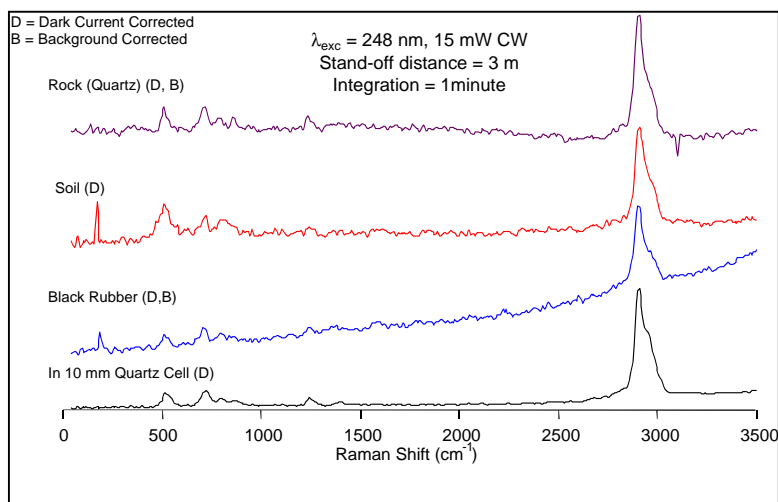


Figure 3. Raman spectra for SF-96 oil on various surfaces for laser excitation at 244 nm.

Of course, in order to identify chemicals in complicated mixtures, it is necessary to establish a library of Raman spectra for surfaces and chemicals. This library must be quickly searched for matches with the measured spectra. While we have developed and tested an adaptive mixing algorithm, which is able to simultaneously determine the mixing coefficients of 12 chemicals in a simulated composite spectrum,¹³ much more work is necessary as it is highly likely that a spectral database useful to a First Responder would contain 100s of chemicals.

Sensitivity Estimate

In estimating the ultimate sensitivity of the MRLS, we assume that the signal-to-noise ratio is limited primarily by the signal shot noise. Hence, it is necessary to verify the operating parameters for which this assumption is valid. One parameter is the size of the signal compared to the inherent detector noise. Variations in detector response and variations in the dark current from one pixel to another (or “fixed pattern noise”) are two forms of detector noise. However, these can be removed by normalizing the signal with respect to the measured pixel response and by subtracting the dark current background from the signal. The real sources of detector noise are the “read out” noise (i.e. noise associated with analog to digital conversion of the signal) and the shot noise associated with the dark current. The read out noise is typically 1 count, while the dark noise is approximately $3.5 \text{ counts} \cdot (\text{Hz})^{1/2}$ when the CCD chip is cooled to -40 C . For one second of signal integration, the RMS noise is approximately 3.7 counts. For signals of this size, the detector noise becomes significant.

Another parameter is the signal integration time or, for a pulsed laser, the number of laser shots. For a shot-noise limited system, the signal-to-noise ratio (SNR) scales with the square root of the integrated signal and, thus, is proportional to the square root of the number of laser shots (N).

$$SNR \propto \sqrt{N}$$

For a log-log plot of SNR vs. N, the relation becomes

$$\text{Log}(SNR) = \frac{1}{2} \text{Log}(N) + \text{Const.},$$

which is simply a straight line with a slope of $1/2$. However, if there are other sources of noise (such as laser speckle) that limit the growth of the signal-to-noise ratio as a function of time, this relationship breaks down.

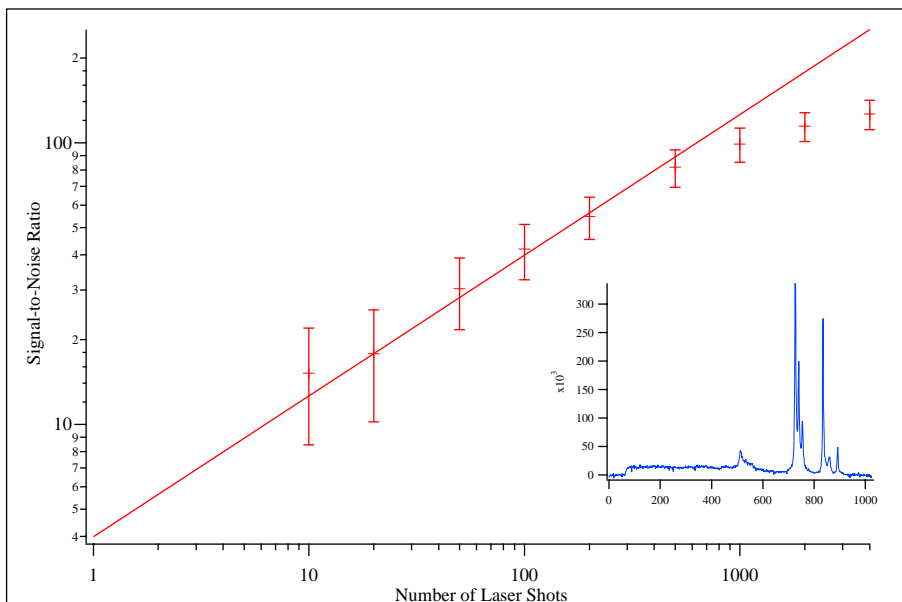


Figure 4. Log-Log plot of signal-to-noise vs. number of laser shots for the 732 cm^{-1} mode of Teflon. The straight line is the dependence in the limit that shot-noise is the only significant noise source. The inset is a Raman spectrum of Teflon. See text for details.

Figure 4 shows the SNR for the 732 cm^{-1} mode of Teflon as a function of laser shots from one shot up to 4,000 shots. For the 20 Hz Nd: YAG laser in the MRLS, this corresponds to a variation in signal integration time from 50 ms to 200 seconds. The SNR is defined as the baseline-corrected area under the 732 cm^{-1} mode divided by the RMS noise of the baseline. Over the first two decades of integration time, the measured SNR follows the characteristic behavior of a system limited by signal shot noise. However, at longer integration times, there appears to be some deviation from the shot noise limit. As the long integration data is preliminary, it will be reexamined to confirm the validity of this deviation. Nonetheless, for the integration times expected for the MRLS in the field (< 1 min), the estimates of sensitivity (both theoretical and empirical) for which shot noise is the dominant noise source appears to still be valid.

For short-range detection of surface or ground contamination, the angle of the laser beam with respect to the normal of the surface is likely to be large (fifty degrees or more). Most of the samples interrogated with the MRLS were illuminated at near normal incidence. To observe the effect of the interrogation angle on the Raman return signals, we have measured the Raman spectrum of a sheet of Teflon. The angle between the laser beam and the normal of the surface was varied from 0° to 75° . The size of the Teflon sheet was large enough to ensure that the laser beam does not overflow it, even at the large angle of incidence. The area under the 732 cm^{-1} peak after one minute of signal interrogation is shown as a function of angle in Figure 5. As is clearly seen, the Raman signal drops by a nearly a factor of seven between incidence at 0° and at 75° . To explain this effect, we have calculated the loss of collected Raman light due to “defocusing”. As the interrogation angle increases, the laser beam spans more of the length of the Teflon sheet. When the receiver telescope forms an image of the illuminated area on the Teflon, the edges of the laser beam are out of focus with respect of the center of the laser beam. For the standoff distance of 2.25 m, this effect can be significant. The depth of focus of the telescope is shorter than it would be for a longer-range lidar receiver. Hence, less of the Raman scattered light is able to pass through the spectrometer slit, and the signal decreases. The solid line in Figure 5 shows a model calculation of the Raman signal strength as a function of interrogation angle (i.e., variations in the slit transmission caused by this defocusing effect). However, as is clearly discernible in this figure, the slit transmission model alone cannot completely explain the angular dependence. It is interesting to note that the remaining differences between the slit model and the experimental data can be reconciled when a Lambertian cosine dependence is combined with the slit transmission model.¹⁴

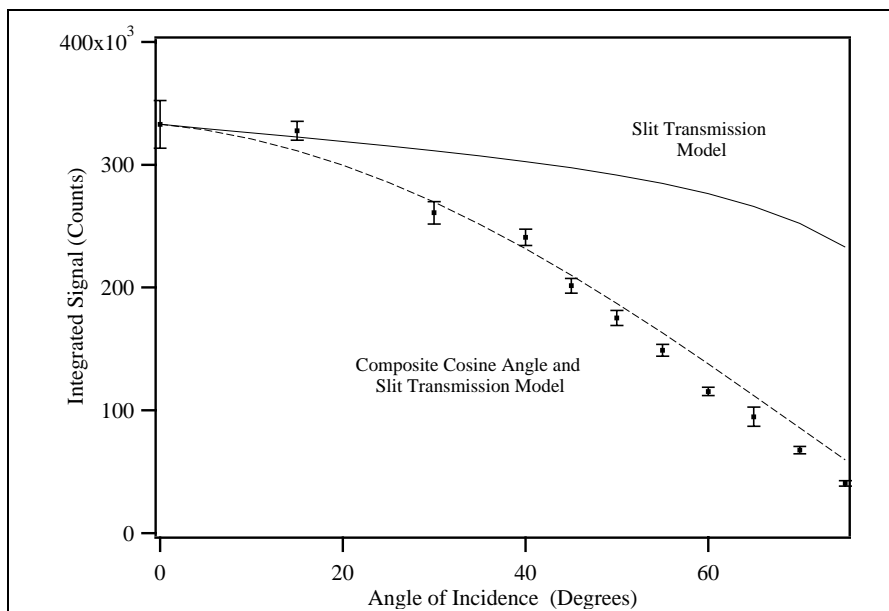


Figure 5. Total area under the 732 cm^{-1} peak of Teflon vs angle-of-incidence between the laser beam and normal of the Teflon surface. The experimental points are shown with their associated error bars. The modeled data are shown by the solid and dashed curves.

In the case of fluorescence within or near the Raman window, a change of laser excitation wavelength can shift the Raman spectrum into a fluorescence-free region. Fluorescence from tryptophan¹⁵, a protein found in many forms of bacteria, is one such important case. The fluorescence maximum is near 370 nm, with the tail extending into the 270-nm-to-300-nm Raman window. A change in laser excitation wavelength by 10 nm to 15 nm to the blue of 266 nm yields a fluorescence-free window for the Raman spectrum. The reason is that the Raman wavelengths follow the change in the laser wavelength, while the wavelength of the fluorescence (which results from a transition between the same electronic states) remains fixed. The result is that the Raman spectrum is “blue-shifted” away from the tail of the tryptophan fluorescence.

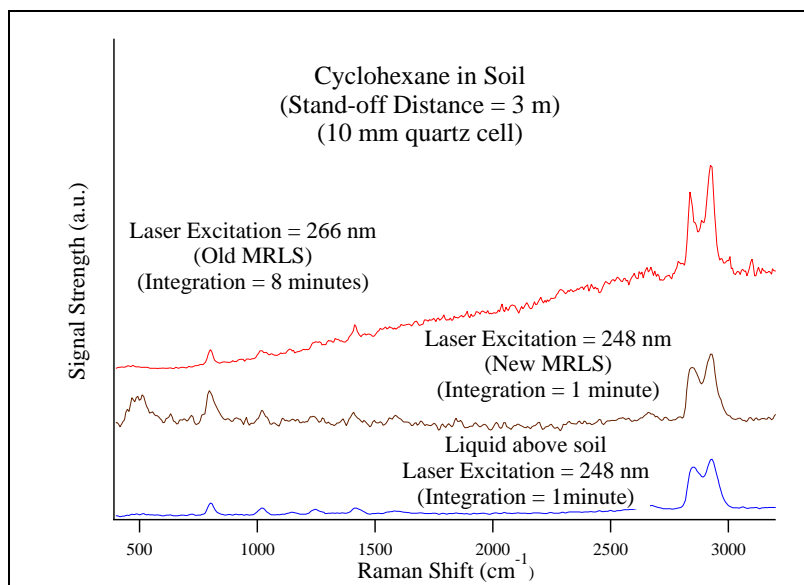


Figure 6. Raman spectra of cyclohexane on soil for laser excitation at 266 nm and 248 nm. (The spectra have been offset for clarity.) Excitation at 248 nm shifts the Raman modes out of the tail of the tryptophan fluorescence. The spectral window for the 248 nm Raman system is narrower than that of the 266 nm system. The Raman shifts (in cm^{-1}) of two modes of cyclohexane are labeled.

Figure 6 illustrates the use of this technique for the solvent cyclohexane poured onto soil. The bottom spectrum is a reference spectrum of pure cyclohexane excited by the 266 nm laser in the MRLS. The top spectrum, also acquired with the MRLS, is from the cyclohexane and soil sample. The MRLS probed only the surface of the sample. The Raman modes of cyclohexane are visible, with the fluorescence from tryptophan as the background. The same sample was then placed into a 248 nm lab-based Raman system. The spectral window of the lab system is narrower than that of the MRLS so that only some of the cyclohexane modes are visible. For 248 nm excitation, the tryptophan background is gone, and the Raman modes of cyclohexane sit on a flat, quiet background. This is an important finding since tryptophan is ubiquitous in the environment. In addition to the improvements in the optical throughput of the MRLS, another goal is the incorporation of a laser source near 250 nm.

In some cases where the surface and/or the contaminants fluoresce within the Raman spectral window, there may be little that can be done to circumvent the effect on the sensitivity. Since Raman scattering is virtually instantaneous compared to fluorescent decay, fast gating of the detector could possibly decrease the detection efficiency of the longer-lived fluorescent background with respect to the prompt Raman signal. However, it is impossible to make a general statement about the usefulness of such a technique. The issue of fluorescence must be addressed on a case-by-case basis.

The LISA Concept

In an effort to transition the MRLS technology from the “proof-of-principle” stage to a field-harden system usable by non-experts, BNL and ITT have been in collaboration on a next generation system referred to as LISA (Laser Interrogation of Surface Agents). The LISA concept is illustrated in Figure 7. A laser transmitter serves as a spectrally narrow light source with high irradiance. It illuminates a chemical agent deposited on a surface. A portion of the incident light is Raman scattered by the chemical compound. This light is scattered both spatially in all directions as well as spectrally into preferred wavelengths corresponding to the unique vibrational energies of the chemical. The Raman scattered light is collected by a telescope and is coupled into a dispersive optical system. In contrast to the MRLS, the telescope focuses the collected light onto an optical fiber bundle. At the opposite end of the fiber bundle, individual fibers are oriented linearly to form an entrance slit for a grating-based spectrograph. A focal plane array detector records the optical spectrum of the Raman scattered light. This spectrum serves as a “fingerprint” for the chemical compound. An analysis computer employs pattern-matching algorithms to identify the chemical from its spectral library of known compounds.

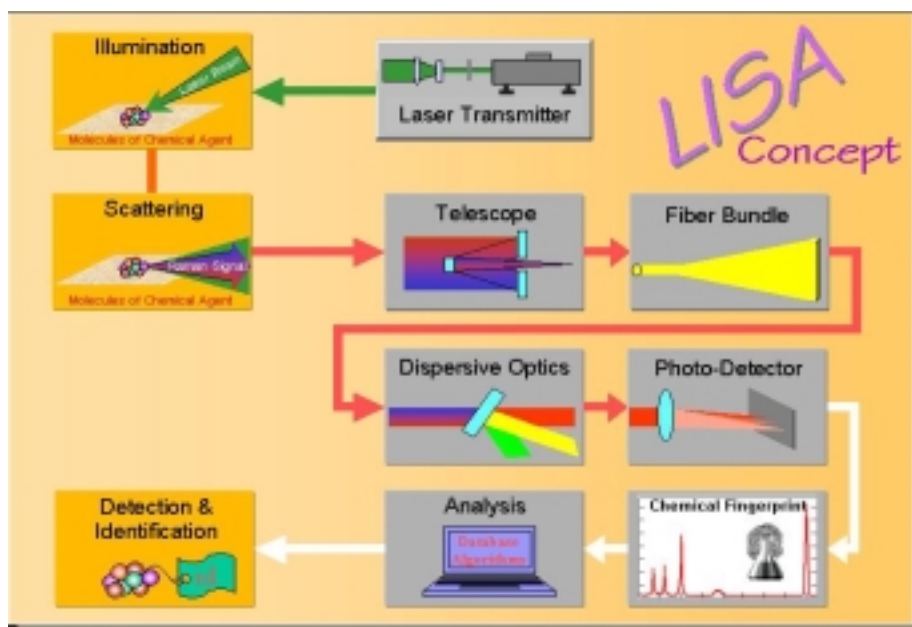


Figure 7. The LISA concept

LISA-Recon Prototype Design

The LISA-Recon prototype has been designed specifically to meet the need of the Army for on-the-move detection of chemical warfare agents. The LISA-Recon system consists of a sensor module, which will be mounted to the rear of the

Nuclear Biological Chemical Reconnaissance Vehicle (NBCRV) and stare at a fixed pointing direction at the ground. The sensor module will be connected by umbilical to an operator's console interior to the vehicle. The control and analysis computer has the capability to analyze a complicated measured spectrum for the presence of chemical agents in real-time for each individual laser shot.

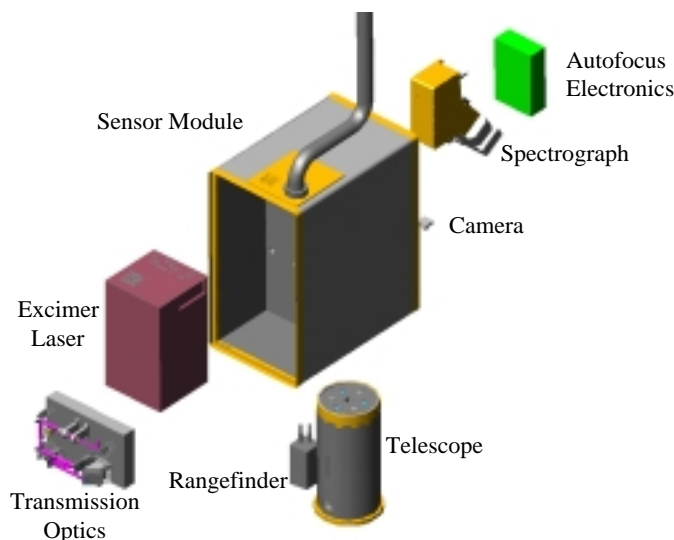


Figure 8. LISA sensor module design.

An exploded view of the sensor module is shown in Figure 8. The sensor module housing provides environmental protection and a rigid mounting surface for the sensor subsystems. In the initial phase of the prototype development effort, a line-narrowed excimer laser will serve as the laser transmitter. This laser is very compact (10"x10"x18") and can produce 20 mJ pulses at 248 nm with a pulse repetition rate of 25 Hz. Concurrently, a frequency-tripled, air-cooled alexandrite laser is being developed to serve as the final field transmitter. The alexandrite laser has the advantage of being an all-solid state source containing no hazardous gases.

Beam shaping and steering optics in front of the laser insure that the laser spot on the ground has the optimal size and is centered in the telescope field of view. The beam is transmitted coaxially with the telescope. The collecting telescope has an 8-inch primary mirror and has been designed for a standoff distance of 1.5 m. Since the reconnaissance vehicle will travel over rough terrain, a fixed focus telescope is not the optimal configuration. The LISA system has been designed with an autofocus telescope system which utilizes a rangefinder to measure the distance to ground, computes the focus position to optimize the optical throughput for the next laser pulse, and holds the telescope focus at this position. It is capable of performing this task for each laser pulse (i.e., 25 times a second).

The telescope is fiber coupled to the analyzing spectrograph. This feature enables the subsystems to be located based upon packaging or mechanical considerations without sacrificing optical alignment tolerances. The spectrograph contains a Raman edge filter (Barr Associates) to reduce the 248-nm excitation energy, a flat grating, and associated focusing optics. The dispersed spectrum is recorded by an intensified CCD array and is read out to the computer after every laser shot. A diagnostic video camera is mounted on the LISA sensor in order to provide further documentation of the interrogated surfaces during field-testing.

Increased optical throughput is the key improvement over the MRLS that will enable single-shot detection at the stipulated sensitivity level. A systematic analysis of each optical component in the MRLS and the LISA prototype design was undertaken in order to estimate the expected improvement in the performance of the LISA-Recon system. The major modifications incorporated into the LISA-Recon system are: (i) reduced wavelength—improves scattering efficiency and reduces bio-fluorescence background, (ii) higher laser energy (20 mJ/pulse), (iii) increased telescope diameter, (iv) increased spectrometer input coupling, and (v) improved detector quantum efficiency. Taking all these factors into account yields an increase in sensitivity of approximately 300 relative to the MRLS.

A performance comparison of the MRLS and LISA-Recon systems relative to the Army's sensitivity requirement is shown in Figure 9. In this figure, the single-shot sensitivity of the MRLS is shown if its standoff distance were 1 m and if it was modified to incorporate a 20 mJ, 248 nm laser.¹⁶ The estimated LISA-Recon sensitivity, a factor of 300 better, is also shown for the same standoff-distance. Since the actual standoff-distance for the LISA-Recon system is 1.5 meters, its expected sensitivity is reduced by a factor of ~2 to 0.015 g/m². This value exceeds the sensitivity requirement by a factor of 30. Also shown in Figure 9 is a solid curve illustrating the variation in detection sensitivity with standoff range for a system with the 0.5 g/m² sensitivity at 1m.

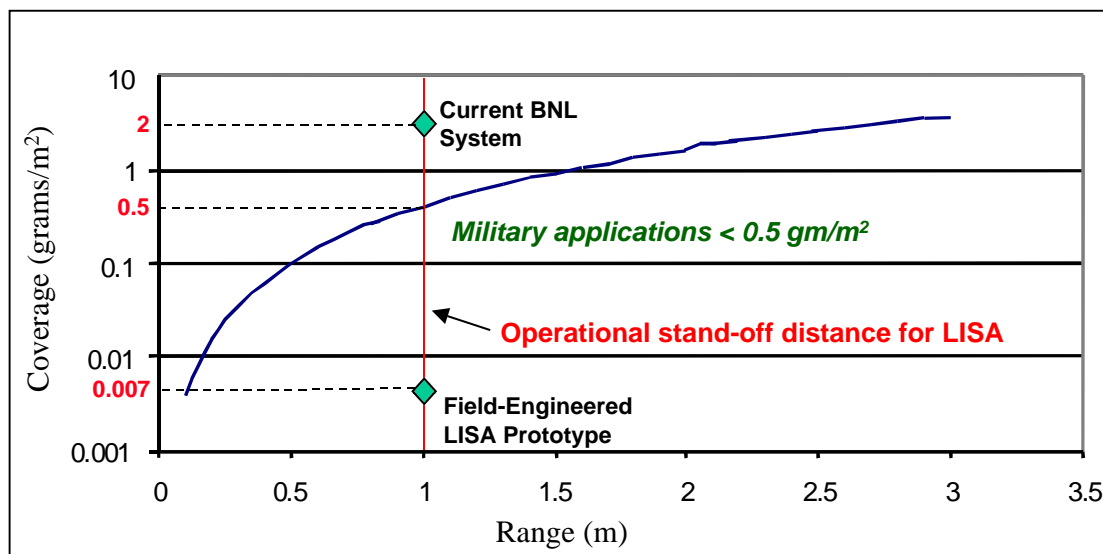


Figure 9. The LISA-Recon system significantly exceeds the required sensitivity for chemical detection.

Future Applications For Military Missions And Homeland Defense

The potential of the LISA-Recon system to provide standoff detection and identification of chemical agents has led to significant interest in additional realizations of MRLS/LISA technology to address other critical military needs, significantly enhance homeland defense and enable rapid response to acts of domestic terrorism. These applications include the inspection of personnel, buildings, equipment and vehicles for chemical contamination, the continuous monitoring of exposed ship decks and superstructures for chemical agents, the use of man portable sensors for detection during special operations, autonomous or remote scanning for contamination with Unmanned Ground Vehicle (UGV) scouts, continuous point monitoring of ventilation systems, and the routine inspection of food.

In addition, MRLS/LISA technology could also be extended to peacetime applications such as HazMat response and the characterization of contaminated industrial sites. Realization of these configurations will significantly enhance the capability of our warfighters and emergency responders to react to a wide variety of suspected occurrences of chemical contamination and to quickly gather the information they require to take the most appropriate action.

Feedback from the chemical and biological defense community has indicated that the most useful configurations of the LISA technology would be a man portable version, an inspection station unit, and a point sensor unit. Organizations responsible for emergency management and domestic response have also emphasized the importance of a man portable or handheld LISA instrument and the need for autonomous, user-friendly operation. A man portable MRLS/LISA sensor would make the technology available to a larger cross section of users and facilitate its application to a much broader range of chemical contamination situations including inside buildings, subways, and other enclosures. Man portable operation will require significant advances in technology such as compact battery-operated lasers, miniaturized high-resolution spectrometers with high etendue, and novel packaging schemes. These same technologies will also be applicable to deployment on a UGV.

Conclusions

The mini-Raman Lidar technology represents a new venue of short-range, standoff surface contamination assessment in the field of lidar. This novel short-range, standoff detection scheme offers the possibility of detecting and uniquely identifying

chemicals on a variety of surfaces, both natural and man-made, without having to collect a sample or come into contact—or even near contact—with the contaminants. This capability has been demonstrated using a proof-of-principle system referred to as the Mini-Raman Lidar System (MRLS). In a follow-on development effort between BNL, ITT and SBCCOM, a next generation MRLS-like instrument known as Laser Interrogation of Surface Agents (LISA) is being developed to provide the capability for standoff detection of chemical agents. The LISA-Recon device is presently being fabricated with subsystem tests to follow in the fall and winter of 2001. Field-testing of the LISA-Recon system will occur during 2002.

Acknowledgements

We wish to acknowledge Mr. David Harder for technical support in constructing the MRLS and Drs. Ming Wu, and Chris Dyer for helpful technical assistance and discussions, respectively. In addition, the authors acknowledge members of ITT and SBCCOM who are making the LISA-Recon prototype system a reality. Our coworkers at ITT include Thomas H. Chyba, Patrick L. Ponsardin, Wayne T. Armstrong, C. Ted Lobb, Brian P. Kelly, Robert Babnick, Quang Bui, Nathan Lucas, Loyd Overbay, Waverly Marsh and David Sanchez. We especially thank the support of personnel from SBCCOM: Lt. Col. Donald Burnett, Arne Johnson, Janice Nordin, Timothy Pedrick, Marty Sennett and Lisa Silks. We also acknowledge technical contributions and advice from Dr. Steve Christesen at the Edgewood Chemical Biological Center, Aberdeen Proving Ground, especially for performing the calculations underlying Figure 7. This effort is jointly funded by ITT Industries, Advanced Engineering and Sciences Division and by SBCCOM through contract DAAD13-01-C-0018. Work performed at Brookhaven National Laboratory was supported by the Department of Energy under Contract No. DE-AC02-98CH10886.

References

1. LIFI, Laser-induced Fluorescence Imager, Special Technology Laboratory, Santa Barbara, CA, private communication.
2. M. Druy, Sensiv Corporation, private communication.
3. H. T. Skinner, T. F. Cooney, S. K. Sharma, and S. M. Angel, *App. Spec.* **50**, 1007 (1996).
4. W. S. Sutherland, J. P. Alarie, D. L. Stokes, and T. Vo-Dinh, *Instrum. Sci. and Technol.* **22**, 231 (1994).
5. S. M. Angel, M. L. Myrick, and T. M. Vess, *Proc. SPIE-Int. Soc. Opt. Eng.* **1435**, 72 (1991)
6. S. H. Lieberman, D. S. Knowles, and P. Poss, Annual Meeting of the Optical Society of America and XI Interdisciplinary Laser Science Conference, Portland, OR, 10-15 September 1995.
7. M. D. Ray and A. J. Sedlacek, "Mini-Raman Laser-Radar System for *In Situ*, Stand-off Interrogation of Surface Contamination", 19th International Laser Radar Conference, July 6-10, 1998, NASA/CP-1998-207671/PT2, p. 677.
8. S. D. Christesen, *Applied Spectroscopy* **42** 318 (1988).
9. S. D. Christesen, "Raman spectroscopy for contamination monitoring," CRDEC-TR-137 (Aberdeen: Aberdeen Proving Ground, Chemical Research Development and Engineering Center) March 1990
10. A. Sedlacek and N.S. Higdon, "Laser interrogation of surface agents: LISA joint chemical field trial test report", DAAD09-00-P-0241, February 22, 2001
11. M. Wu, M. D. Ray, K. H. Fung, M. W. Ruckman, D. Harder, and A. J. Sedlacek, *Applied Spectroscopy* **54**, 800 (2000).
12. J. M. Dudik, C. R. Johnson, and S. A. Asher, *J. Chem. Phys.* **82**, 1732 (1985).
13. D.J. Burr, C. L. Chen, and A.J. Sedlacek, SPIE 1996 International Symposium on Optical Science, Engineering and Instrumentation, Denver, CO, August 4-9, 1996.
14. Dr. Chris Dyer, Defence Science and Technology Laboratory (DSTL)/UK, private communication.
15. S. Chadha and W.H. Nelson, *Rev. Sci. Instrum.* **64**, 3088 (1993).
16. The sensitivity calculations for the modified MRLS and the variation in sensitivity with standoff distance shown in Figure 9 were performed by Dr. Steve Christesen, Edgewood Chemical Biological Center, Aberdeen Proving Ground.